INTERNATIONAL JOURNAL FOR NUMERICAL METHODS IN FLUIDS, VOL. 21, 1007–1014 (1995)

MASSIVELY PARALLEL FINITE ELEMENT ANALYSIS OF COUPLED, INCOMPRESSIBLE FLOWS: A BENCHMARK COMPUTATION OF BAROCLINIC ANNULUS WAVES

QIANG XIAO, ANDREW G. SALINGER, YUMING ZHOU AND JEFFREY J. DERBY*

Department of Chemical Engineering and Materials Science and Army High Performance Computing Research Center, University of Minnesota, Minneapolis, MN 55455-0132, U.S.A.

SUMMARY

Coupled, three-dimensional, time-dependent, incompressible flows in a differentially heated, rotating annulus are simulated using a parallel implementation of the Galerkin finite element method on the Connection Machine 5 (CM-5) supercomputer. The development of baroclinic annulus waves is computed and found to be consistent with previous experimental reseults. The implementation of a repeated spectral bisection element-partitioning technique significantly increases the computation speed over a strategy which randomly maps elements to processors, yielding sustained calculation rates of 8·1 GFLOPS on 512 processors of the CM-5.

KEY WORDS: finite element; massively parallel; coupled flow; baroclinic annulus waves

1. INTRODUCTION

Massively parallel computing platforms and algorithms hold great promise for analysing a spectrum of issues involving fluid mechanics and transport phenomena, especially in systems where three-dimensional and time-dependent behaviours predominate. In this paper we present the results from a benchmark calculation of a classical fluid flow, baroclinic annulus waves, which is representative of the coupled flows found in many material-processing systems of interest to us.[1] Our specific interests centre on processes employed to produce advanced materials such as large, single crystals for photonic and electronic devices[2–5] and ceramic materials.[6,7] Such processes are characterized by complex geometries which are often time-dependent, coupled incompressible flows, heat and mass transfer, chemical reaction and phase change.

An excellent example of a material-processing system which exhibits three-dimensional flows is the Czochralski method for the growth of large, single crystals. This technique is employed to manufacture most of the world's supply of single-crystal silicon as well as many other technologically important crystals such as gallium arsenide and various refractory oxides.[8] In this method a single crystal is pulled from the surface of a molten material contained in a crucible. This melt is subjected to buoyant forces due to temperature gradients through the system and to rotational forces from the crystal, which is slowly spun while being pulled. Numerous researchers have experimentally observed three-dimensional flow structures in real and model Czochralski melts.[9–13]

Towards our goal of simulating coupled, three-dimensional, transient flows in material-processing systems, we choose a benchmark simulation of the classical system of a fluid-filled annulus which is rotated and differentially heated.[14–16] This system has long been employed experimentally to study the

*Author to whom correspondence should be addressed.

CCC 0271–2091/95/101007–080

Received 19 August 1994
Revised 1 November 1994

essential physical attributes of large-scale atmospheric circulation[17] and has also been employed to study non-linear structures in flows and the onset of chaotic behaviour in fluid systems.[18] This simple system exhibits a wide range of complicated flows which arise from the non-linear interactions between the Coriolis force induced by system rotation and the buoyancy induced by lateral temperature gradients. For low rotation rates the flows are axisymmetric; however, at a critical rotation rate these flows undergo a transition caused by the baroclinic instability[19] to form a pattern of annular wave-like structures. At even higher rotation rates and temperature gradients these structures can vacillate periodically in time or can form irregular, chaotic patterns.

While this system is rich in its display of complicated fluid dynamical phenomena, we again emphasize its employment here primarily as a benchmark for our code. Previous numerical simulations of flow in a rotating, differentially heated annulus include the two-dimensional, finite difference calculations of Williams.[20,21] Williams extended his study to the three-dimensional flow structure of azimuthal wave number five using a finite difference scheme.[22] More recent attempts at the calculation of the three-dimensional flows in this system include the mixed spectral and finite difference approach of Quon[23] and the pseudospectral algorithm developed by Le Quéré and Pécheux.[24] We approach the simulation of this system using a massively parallel implementation of the Galerkin finite element method. Our initial efforts in developing this algorithm were reported in Reference 25; subsequent code modifications and the performance of this approach in the calculation of baroclinic annulus waves are reported in the following sections.

2. PROBLEM FORMULATION

We consider a differentially heated, fluid-filled annulus of rectangular cross-section which rotates around its symmetric axis; see Figure 1. We consider a Cartesian co-ordinate system fixed to the symmetric axis of the system and write the dimensionless, rotational form[15] of the Navier–Stokes equation with the Boussinesq approximation for an incompressible fluid, along with the energy balance equation, as

$$\frac{\partial \mathbf{v}}{\partial t} + \mathbf{v}\cdot\nabla\mathbf{v} - 2PrRe(v_y\mathbf{e}_x - v_x\mathbf{e}_y) = \nabla\cdot\boldsymbol{\sigma} - GrPr^2FrT(x\mathbf{e}_x + y\mathbf{e}_y) + GrPr^2T\mathbf{e}_z, \tag{1}$$

$$\nabla\cdot\mathbf{v} = 0, \tag{2}$$

$$\frac{\partial T}{\partial t} + \mathbf{v}\cdot\nabla T = \nabla^2 T. \tag{3}$$

The stress tensor $\boldsymbol{\sigma}$ is defined as

$$\boldsymbol{\sigma} = -P\mathbf{I} + Pr(\nabla\mathbf{v} + \nabla\mathbf{v}^{\mathrm{T}}). \tag{4}$$

The dimensionless variables are defined as follows: $\mathbf{v}$ is the flow velocity (scaled by α/R), T is the temperature (scaled by the temperature difference ΔT), t is the time (scaled by R^2/α), P is the pressure (scaled by $\rho\alpha^2/R^2$), $\mathbf{e}_x$, $\mathbf{e}_y$ and $\mathbf{e}_z$ are unit vectors along the axes x, y and z respectively, $\mathbf{I}$ is the identity tensor and the superscript T denotes the transpose operation. The radius of the outer cylindrical wall, R is chosen as the characteristic length scale and the thermal diffusivity α is defined as $\alpha = k/\rho C_{\mathrm{p}}$, where k is the thermal conductivity, ρ is the density and C_{p} is the specific heat of the fluid. The dimensionless Grashof number (Gr), rotational Reynolds number (Re), Prandtl number (Pr) and Froude number (Fr)

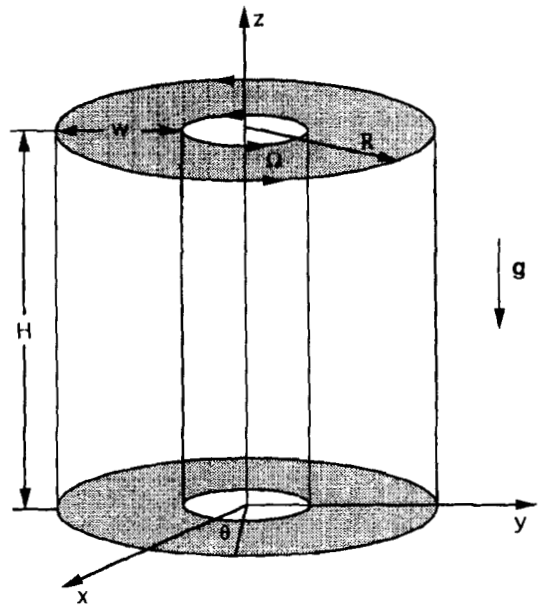

Figure 1. Geometry considered in this study, consisting of a fluid-filled annulus of rectangular cross-section which is laterally heated and rotated around its symmetric axis

are defined as

$$Gr = \frac{\rho^2 R^3 g \beta \Delta T}{\mu^2}, \tag{5}$$

$$Re = \frac{\rho R^2 \Omega}{\mu}, \tag{6}$$

$$Pr = \frac{\mu C_p}{k}, \tag{7}$$

$$Fr = \frac{\Omega^2 R}{g}, \tag{8}$$

where μ is the fluid viscosity, g is the gravitational acceleration, β is the thermal expansion coefficient and Ω is the angular velocity of annulus rotation.

No-slip boundary conditions are applied for the flow field along all surfaces. The warm outer cylindrical wall and the cool inner wall are held at constant temperatures; their difference is denoted by ΔT. The upper and lower surfaces of the annulus are taken to be adiabatic.

3. METHODOLOGY

3.1. Numerical approach

The Galerkin finite element method[26] is used to spatially discretize the above equations. Since we are interested in computing flows of only moderate intensity, stabilization techniques for the advection

terms are not employed. We employ a standard mixed interpolation scheme[27] in which the velocity and temperature fields are expressed as linear combinations of Lagrangian triquadratic polynomials Φ^i with 27 nodes per hexahedral element while the pressure is approximated by a sum of discontinuous linear basis functions Γ^i with four degrees of freedom per element:

$$\begin{bmatrix} v_x(x,y,z,t) \\ v_y(x,y,z,t) \\ v_z(x,y,z,t) \\ T(x,y,z,t) \end{bmatrix} = \sum_{i=1}^{N} \begin{bmatrix} v_x^{(i)}(t) \\ v_y^{(i)}(t) \\ v_z^{(i)}(t) \\ T^{(i)}(t) \end{bmatrix} \Phi^i(x,y,z), \tag{9}$$

$$P(x,y,z,t) = \sum_{i=1}^{N_p} P^{(i)}(t)\Gamma^i(x,y,z), \tag{10}$$

where N is the total number of nodes and N_p is the number of pressure unknowns.

We apply the Galerkin procedure in the standard manner to produce weak-form weighted residual equations. Boundary conditions are invoked using routine finite element procedures.[26] The weighted residual equations are evaluated numerically using 27-point Gauss quadrature on each element to yield a large set of differential–algebraic equations which we denote as

$$\mathbf{M}\frac{\mathrm{d}\mathbf{q}}{\mathrm{d}t} = \mathbf{F}(\mathbf{q}), \tag{11}$$

where $\mathbf{M}$ is the mass matrix, $\mathbf{q}$ is the vector of time-dependent unknowns comprising the complete set of velocity temperature and pressure interpolants and $\mathbf{F}$ is the right-hand side resulting from the spatial discretization of the original partial differential equations. More details of this formulation are available in Reference 28.

Equation (11) is temporally discretized using the backward Euler method, which yields the non-linear equation set

$$\mathbf{M}\frac{\mathbf{q}^{n+1} - \mathbf{q}^n}{\Delta t} = \mathbf{F}(\mathbf{q}^{n+1}), \tag{12}$$

where the superscripts denote the time step and Δt is the step size. This set of equations is then solved using the iterative Newton–Raphson method, resulting in the solution of large linear equation sets at each time step. A constant time step size is employed for the calculations presented here.

3.2. Parallel implementation

The algorithm described above is implemented on the Thinking Machines Corporation Connection Machine 5 (CM-5), a distributed memory, multiple-processor supercomputer. For the sake of brevity we present only the most essential aspects of the parallel implementation here. Interested readers should consult Reference 25 for more details.

The major characteristics of the CM-5 are its large distributed memory and many processors. In order to effectively exploit these features, individual elements are mapped to processors and the element-level components of the residual equations and Jacobian matrix (which arise from the Newton–Raphson iterations performed at every time step) are calculated concurrently. When these computations are complete, the GMRES (generalized minimal residual) iterative scheme of Saad and Schultz[29] is used with diagonal preconditioning to solve the linear algebraic system. We have employed 375 GMRES iterations for each linear equation set solution of the Newton iteration (15 restart loops and a Krylov subspace dimension of 25). To take advantage of the local data structure

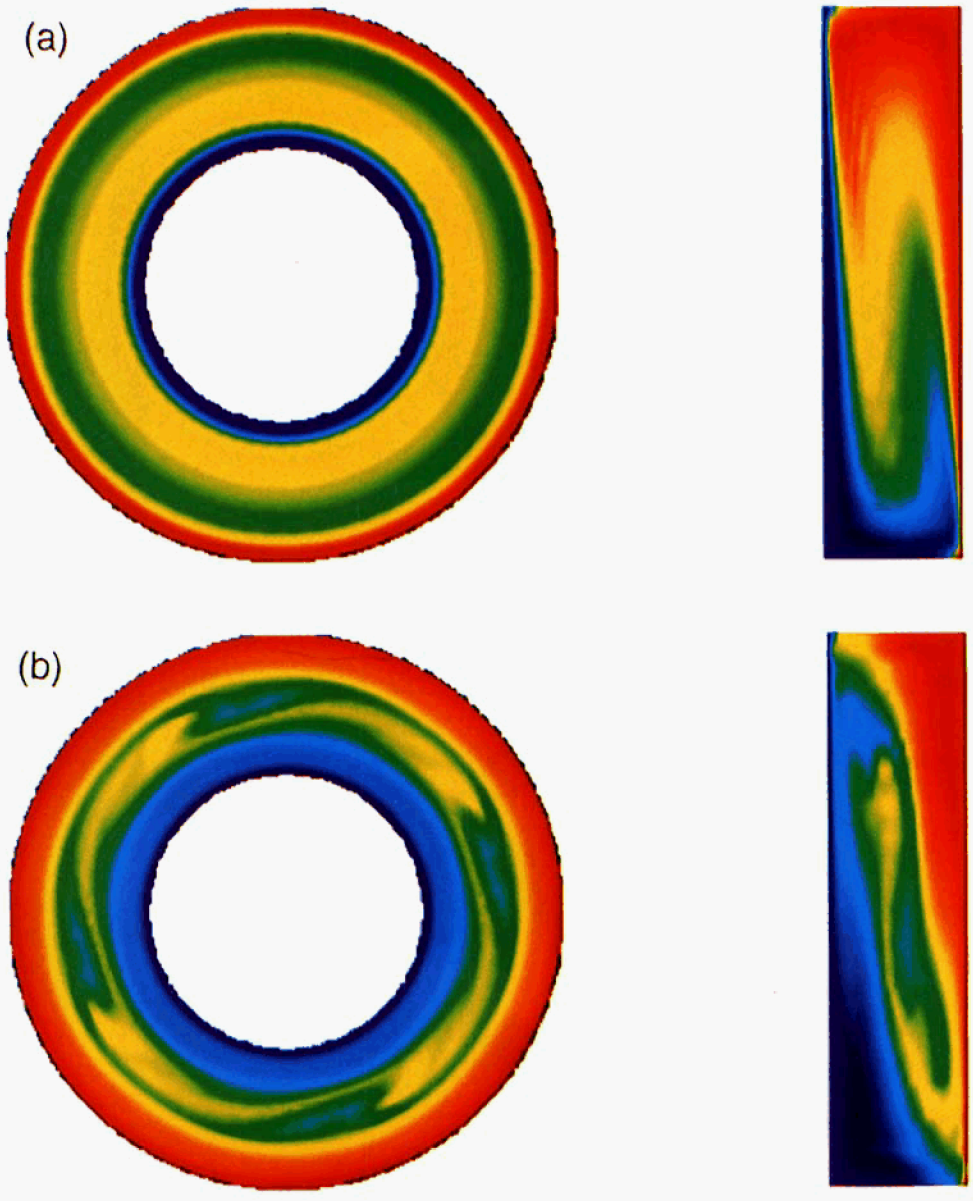

Plate 1. Transient, three-dimensional calculations of the development of a baroclinic annulus wave. The temperature field is represented using a top view, cut through the $z = {}^1/_2\, H$ plane, and a side view through the $\theta = 0$ plane. The colour map for the temperature field is shown in lieu of the side view in case (d). (a) The initial condition is steady, axisymmetric convection in the absence of rotation. (b) The development and growth of annular vortices occurs shortly after the introduction of system rotation. (c) At long times the system exhibits fully developed baroclinic annulus waves. (d) At even longer times the structure of the annular vortices continues to evolve

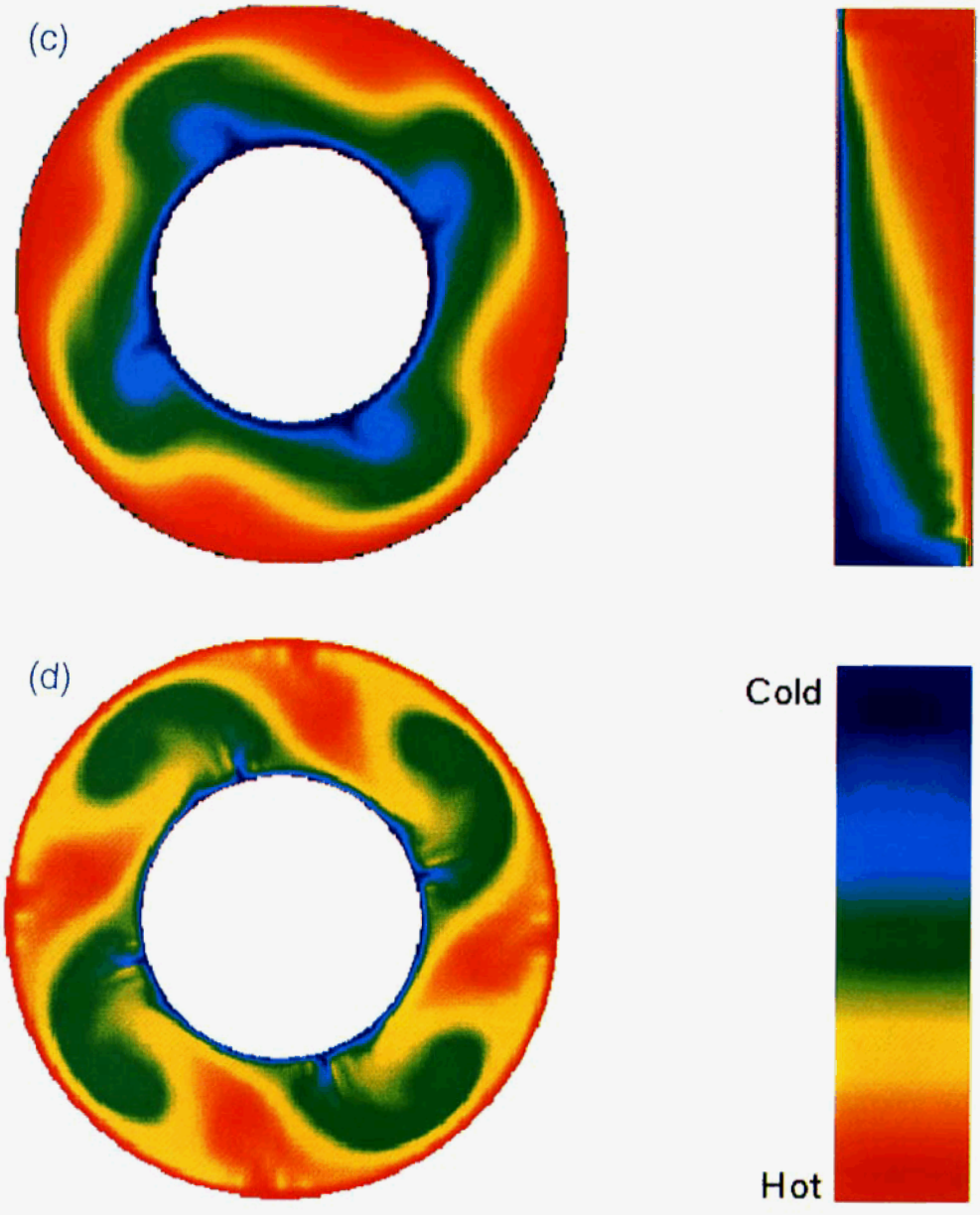

Plate 1. (c), (d) For description see over

described above, the matrix–vector multiplications of GMRES are conducted with element-level rather than global residual and Jacobian matrix elements. Therefore only the resulting update vectors need to be mapped to the global level.[25] This general approach has been used with great effectiveness by Tezduyar and co-workers[30–32] and Johan *et al.*[33] in similar massively parallel implementations of the finite element method.

The cost of communicating between the local and global levels (scattering and gathering) is a function of the positions of the elements with respect to each other on the processors. Our initial approach assigned the elements to processors in a completely arbitrary manner.[25] In the calculations performed here, we endeavour to reduce the communications overhead by partitioning the elements into groups and selectively mapping them to the processors. This task is fulfilled using a recursive spectral bisection procedure[34,35] which is conveniently implemented through the routine '*partition_mesh*' of the CM-5 scientific library (CMSSL). The performance increase as a result of this element partitioning will be reported in Section 4.2.

4. RESULTS

A schematic diagram of the system geometry is shown in Figure 1. We choose conditions to mimic the experimental apparatus employed by Koschmieder.[16] The radius of the outer cylindrical wall is set to be 5 cm, with a gap thickness of 2·5 cm. The height of the annulus is 10 cm. The thermophysical properties of water are employed and a temperature difference of 10°C is applied across the gap. The rotation rate is set to be $\Omega = 2{\cdot}5$ rad s^{-1}. The dimensionless parameters for these calculations are then $Gr = 2{\cdot}54 \times 10^6$, $Re = 6{\cdot}25 \times 10^3$, $Pr = 6{\cdot}96$ and $Fr = 3{\cdot}18 \times 10^{-2}$. Figure 2 shows the finite element mesh employed for our computations, which consists of 20,480 triquadratic elements with a total of 774,656 mathematical unknowns.

4.1. Baroclinic annulus waves

A steady flow calculated for a system with no rotation is employed as the initial condition in our system. The temperature field corresponding to this flow is shown in Plate 1(a). The flow is

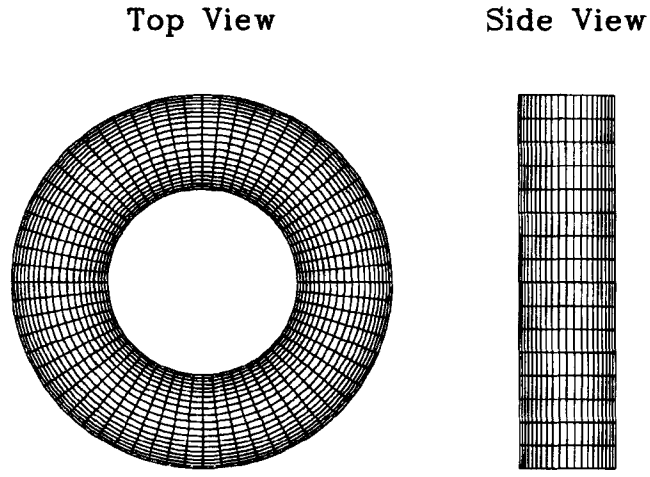

Figure 2. Top and side views of finite element mesh used for computations described in Section 4. The mesh consists of 20,480 triquadratic elements with a total of 774,656 mathematical unknowns

axisymmetric and driven solely by buoyancy. Warm fluid rises near the outer wall and descends along the cool inner wall. The distorted temperature field shown in the side view clearly indicates the convective nature of the flow.

The simple axisymmetric flow of Plate 1(a) becomes unstable to azimuthal perturbations and gives way to a non-axisymmetric wavy pattern soon after system rotation is introduced. This developing structure is seen in Plate 1(b) and exhibits a dominant azimuthal wave number of four. The distorted temperature field seen from the top view has a distinct fourfold symmetry.

At much longer times the fully developed wave structure becomes evident; see Plate 1(c). Eight flow cells (four clockwise and four counterclockwise) are aligned vertically and rotate at nearly the same rate as the container (they are nearly stationary in the rotating frame of reference of the calculation). The flows across the annulus are now much weaker than the corresponding flows of the axisymmetric case shown in Plate 1(a), as indicated by the less distorted isotherms in the side view.

The flow continues to evolve, with the annular vortices strengthening, as shown in Plate 1(d). Although it is difficult to discern solely from the temperature field, a more detailed analysis of this flow reveals significant changes in the shapes of the annular vortices; the four vortices with clockwise circulation appear to be pinching into eight flow cells. Continued temporal evolution of this flow will likely result in significant changes in its spatial and temporal character; quasi-periodic and chaotic flow regimes have been observed in experiments.[18]

Koschmieder[16] observed very similar flows with azimuthal wave number four in his experiments under the same conditions as employed in our calculations. Such agreement corroborates the veracity of our algorithm and its implementation. While other three-dimensional structures have been observed under different conditions,[14–24] we have not actively pursued the computation of these flows.

4.2. Code performance

An analysis of code performance is presented in Table I. All calculations were performed using 64 bit precision arithmetic on 512 processors of the CM-5 of the Army High Performance Computing Research Center at the University of Minnesota. Speeds are reported in GFLOPS (billions of floating point operations per second), which were calculated from the elapsed time and the number of floating point operations indicated in the assembly language listing generated by the compiler. For the performance test conducted here, a larger system of 32,768 triquadratic elements and 1,212,672 total degrees of freedom was employed in order to directly compare with our previous implementation.

Table I. Performance results obtained with 512 processors of CM-5 for one Newton–Raphson iteration during coupled, incompressible flow calculations described in text. Results are indicated for implementations without (w/o P.) and with (w/P.) element partitioning*

Programme section	Floating point operations	Time (s)		Speed (GFLOPS)	
		w/o P.	w/P.	w/oP.	w/P.
Evaluation of residual and Jacobian	118×10^9	12·4	12·4	9·5	9·5
GMRES solution (total)	330×10^9	62·0	42·8	5·3	7·7
375 matrix–vector multiplications	309×10^9	20·5	20·5	15·1	15·1
375 scatters+375 gathers	0	35·5	16·3	0	0
Sustained rate	448×10^9	74·4	55·2	6·0	8·1

*These results were obtained using a beta test version of the CM-5 software and consequently are not necessarily representative of the performance of the full version of this software.

The calculations performed here feature the element-partitioning scheme described above to reduce communications overhead; Table I compares current code performance results with those of our prior implementation without element partitioning.[25] The speeds of residual and Jacobian evaluation (9·5 GFLOPS) and matrix–vector multiplications within GMRES (15·1 GFLOPS) are not affected by element partitioning. However, the current implementation more than doubles the communication speed between local and global data structures (through the 375 scatters and gathers during a GMRES solution), thereby more than halving the idle time of the processors. As a result, the sustained rate of the calculations is increased from 6·0 to 8·1 GFLOPS.

5. CONCLUSIONS

The coupled, three-dimensional, time-dependent, incompressible flows in a laterally heated, rotating annulus are successfully computed using a parallel implementation of the Galerkin finite element method. The evolution of baroclinic annulus waves with a fourfold azimuthal structure is simulated and found to be consistent with experimental results.

The newly implemented element-partitioning technique, which selectively maps elements to processors using a recursive spectral bisection procedure, more than doubles the speed of communications between local and global data structures and results in a sustained rate of 8·1 GFLOPS on 512 processors of the CM-5. This represents a substantial (approximately 35%) increase in performance over our previous implementation[25] which randomly mapped elements to processors. Interestingly, the relative increase in sustained calculation rate obtained here is less than that obtained by others using the same element-partitioning technique; see Reference 34. This is a consequence of our use of triquadratic elements rather than trilinear elements used by others. More degrees of freedom are contained within the higher-order elements, which results in a more localized elemental data set. This by itself reduces the number and length of communication paths needed between the elemental and global data structures. The communications overhead reduction achieved by partitioning is therefore comparatively less important for our implementation using higher-order elements.

These results demonstrate the great promise for high-resolution computations of three-dimensional, time-dependent flows in realistic systems using massively parallel implementations of finite element methods. Further algorithmic development is needed, especially in improved preconditioners for use with GMRES in the calculation of incompressible flows.[25] However, these techniques are currently enabling significant advances in the study of realistic material-processing systems[36,37] and will undoubtedly promote great advances in analysis via large-scale numerical simulation.

ACKNOWLEDGEMENTS

This work was supported in part by the University of Minnesota Army High Performance Computing Research Center (under the auspices of Army Research Office contract DAAL03-89-C-0038), the Minnesota Supercomputer Institute and the National Science Foundation.

REFERENCES

1. J. J. Derby, S. Brandon, A. G. Salinger and Q. Xiao, 'Large-scale numerical analysis of materials processing systems: high-temperature crystal growth and molten glass flows', *Comput. Methods Appl. Mech. Eng.*, **112**, 69–89 (1994).
2. J. J. Derby, 'Theoretical modeling of Czochralski crystal growth', *MRS Bull.*, **XIII**, (10), 29–35 (1988).
3. J. J. Derby, L. J. Atherton and P. M. Gresho, 'An integrated process model for the growth of oxide crystals by the Czochralski method', *J. Cryst. Growth*, **97**, 792–826 (1989).
4. S. Brandon and J. J. Derby, 'Heat transfer in vertical Bridgman growth of oxides: effects of conduction, convection, and internal radiation', *J. Cryst. Growth*, **121**, 473–494 (1992).

5. Q. Xiao and J. J. Derby, 'Heat transfer and interface inversion during the Czochralski growth of yttrium aluminum garnet and gadolinium gallium garnet', *J. Cryst. Growth*, **139**, 147–157 (1994).
6. J. I. Martinez-Herrera and J. J. Derby, 'An analysis of capillary-driven viscous flows during the sintering of ceramic powders', *AIChE J.*, **40** (11), 1794–1803 (1994).
7. J. I. Martínez-Herrera and J. J. Derby, 'Viscous sintering of spherical particles via finite element analysis', *J. Am. Ceram. Soc., AIChE J.*, **78** [3], 645–649 (1995).
8. D. T. J. Hurle, *Crystal Pulling from the Melt*, Springer, Berlin, 1994.
9. C. D. Brandle, 'Simulation of fluid flow in $Gd_3Ga_5O_{12}$ melts', *J. Cryst. Growth*, **42**, 400–404 (1977).
10. C. D. Brandle, 'Flow transitions in Czochralski oxide melts', *J. Cryst. Growth*, **57**, 65–70 (1982).
11. A. D. W. Jones, 'Flow in a model Czochralski oxide melt', *J. Cryst. Growth*, **94**, 412–432 (1989).
12. K. Kakimoto, M. Watabe, M. Eguchi and T. Hibiya, 'Ordered structure in non-axisymmetric flow of silicon melt convection', *J. Cryst. Growth*, **126**, 2551–2555 (1993).
13. Y. Kishida, M. Tanaka and H. Esaka, 'Appearance of a baroclinic wave in Czochralski silicon melt', *J. Cryst. Growth*, **130**, 75–84 (1993).
14. R. Hide, 'On the dynamics of rotating fluids and related topics in geophysical fluid dynamics', *Bull. Am. Meteorol. Soc.*, **47**, 873–885 (1966).
15. H. P. Greenspan, *The Theory of Rotating Fluids*, Cambridge University Press, London, 1968.
16. E. L. Koschmieder, 'Convection in a rotating laterally-heated annulus', *J. Fluid Mech.*, **51**, 637–656 (1972).
17. P. L. Read, 'The dynamics of rotating fluids: the 'philosophy' of laboratory experiments and studies of the atmospheric general circulation', *Meteorol. Mag.*, **117**, 35–45 (1988).
18. P. L. Read, M. L. Bell, D. W. Johnson and R. M. Small, 'Quasi-periodic and chaotic flow regimes in a thermally-driven, rotating fluid annulus', *J. Fluid Mech.*, **238**, 599–632 (1993).
19. E. T. Eady, 'Long waves and cylcone waves', *Tellus*, **1**, 33–52 (1949).
20. G. P. Williams, 'Thermal convection in a rotating fluid annulus: Part 1. The basic axisymmetric flow', *J. Atmos. Sci.*, **24**, 144–161 (1967).
21. G. P. Williams, 'Thermal convection in a rotating fluid annulus: Part 2. Classes of axisymmetric flow', *J. Atmos. Sci.*, **24**, 162–174 (1967).
22. G. P. Williams, 'Baroclinic annulus waves', *J. Fluid Mech.*, **49**, 417–449 (1971).
23. C. Quon, 'A mixed spectral and finite difference model to study baroclinic annulus waves', *J. Comput. Phys.*, **20**, 442–479 (1976).
24. P. Le Quéré and J. Pécheux, 'A three-dimensional pseudo-spectral algorithm for the computation of convection in a rotating annulus', *Comput. Methods Appl. Mech. Eng.*, **80**, 261–271 (1990).
25. A. G. Salinger, Q. Xiao, Y. Zhou and J. J. Derby, 'Massively parallel finite element computations of three-dimensional, time-dependent, incompressible flows in materials processing systems', *Comput. Methods Appl. Mech. Eng.*, **19**, 139–156 (1994).
26. T. J. R. Hughes, *The Finite Element Method*, Prentice-Hall, Englewood Cliffs, NJ, 1987.
27. P. M. Gresho, 'Contribution to Von Karman Institute lecture series on computational fluid dynamics: advection–diffusion and Navier–Stokes equations', *UCRL-92275*, Lawrence Livermore National Laboratory, Livermore, CA, 1985.
28. Q. Xiao, 'Numerical simulations of Czochralski growth of single crystals', *Ph.D Thesis*, Department of Chemical Engineering and Materials Science, University of Minnesota, Minneapolis, MN, 1994.
29. Y. Saad and M. H. Schultz, 'GMRES: a generalized minimal algorithm for solving nonsymmetric linear systems', *SIAM J. Sci. Stat. Comput.*, 7, 856–869 (1986).
30. T. E. Tezduyar, M. Behr, S. Mittal and A. Johnson, 'Computation of unsteady incompressible flows with the stabilized finite element methods—space–time formulations, iterative strategies, and massively parallel implementations', in P. Smolinski, W. K. Liu, G. Hulbert and K. Tamma (eds.), *New Methods in Transient Analysis*, AMD Vol. 143, ASME, New York, 1992, pp. 7–24.
31. M. Behr, A. Johnson, J. Kennedy, S. Mittal and T. E. Tezduyar, 'Computation of incompressible flows with implicit finite element implementations on the Connection Machine', *Comput. Methods Appl. Mech. Eng.*, **108** 99–118 (1993).
32. M. Behr and T. E. Tezduyar, 'Finite element solution strategies for large-scale flow simulations', *Comput. Methods Appl. Mech. Eng.*, **112**, 3–24 (1994).
33. Z. Johan, T. J. R. Hughes, K. K. Mathur and S. L. Johnsson, 'A data parallel finite element method for computational fluid dynamics on the Connection Machine system', *Comput. Methods Appl. Mech. Eng.*, **99**, 113–134 (1992).
34. Z. Johan, 'Data parallel finite element techniques for large-scale computational fluid dynamics', *Ph.D. Thesis*, Department of Mechanical Engineering, Stanford University, 1992.
35. A. Pothen, H. D. Simon and L. Wang, 'Spectral nested dissection', *Tech. Rep. RNR-92-003*, NASA Ames Research Center, Moffet Field, CA, 1992.
36. Q. Xiao and J. J. Derby, 'Three-dimensional melt flows in Czochralski oxide growth: high-resolution, massively parallel, finite element computations', *J. Cryst. Growth*, **152**, 169–181 (1995).
37. Y. Zhou and J. J. Derby, 'Three dimensional flows in solution crystal growth', *J. Cryst. Growth*, submitted.